

Importance of Carbon Porosity for Energy-Related Applications

T.J. Bandoz

Department of Chemistry and Biochemistry, The city College of New York,
New York, NY 10031, USA

Article info

Received:
15 November 2018

Received in revised form:
27 January 2019

Accepted:
17 March 2019

Abstract

Nanoporous carbons have many advantages over other adsorbents. This includes their high surface area, pore volume and also conductivity of a carbon matrix. The latter is very important for electrocatalysis. In recent years carbon materials have gained a lot of attention as metal-free catalysts. Their catalytic centers have been linked mainly to nitrogen and sulfur heteroatoms incorporated to the carbon matrix. So far, the research efforts have focused mainly on nanoforms of carbons such a graphene and carbon nanotube (CNT). Inspired by those results, we have performed CO₂ and O₂ electroreduction on nanoporous carbons assuming that small pores, similar in sizes to target molecules, can enhance the efficiency of these catalytic processes. Indeed, the results suggested that even though the N- and S- based catalytic centers are important, adsorption of O₂ or CO₂/CO₂/CO/H₂ in pores has a positive effect on these overall reduction processes. This minireview summarizes our recent results on the role of porosity in electrocatalysis on porous carbons.

1. Introduction

Activated carbons, recently referred to as nanoporous carbons, have a long history of applications as adsorbents of gases and liquids, which started with first patents of charcoal activation filled at the beginning of the last century [1–3]. The timing of that invention was very important since, as a result of it, thousands of lives of WWI soldiers were saved by the application of carbons in gas masks against first chemical warfare agents used at that time. Since then activated carbons have been significantly improved by using more advanced activation methods and new methods of their surface modifications by impregnation and doping procedures [4]. Nevertheless, even with all new approaches some features of these materials remain the same and are still their assets. They are a developed surface area and porosity. The pore sizes of carbon can vary from fraction of nanometer in carbon molecular sieves to large micrometer sizes in carbon foams. In recent years, by a template carbonization of various organic precursors the

porous carbons gained the feature of the ordered structure in the range of nanopores/mesopores [5].

Recent developments in porous carbon science have not been dictated by the needs of the separation/adsorption processes, although the latter recently have required sophisticated materials to meet the environmental protection and energy efficiency standards. Thus, many modifications/improvements of porous carbon's surface features were stimulated by their applications beyond adsorption in energy related fields, such as supercapacitors [6], oxygen reduction reaction (ORR) or oxygen evolution reaction (OER) electrocatalyst for fuel cells [7] or CO₂ reduction catalysts [8]. In all these applications, besides specific chemistry determining centers as those based on nitrogen or sulfur [9], pores and their pores sizes were indicated as important [10, 11]. Here, interface target molecule/ion- carbon surface interactions, even though sometimes no directly linked to adsorption, belong to the category of an adsorption process in the general meaning of this word [12]. Classical examples are supercapacitors where the pores of species sizes were found as very important for an efficient energy storage [10, 11].

*Corresponding author. E-mail: tbandosz@ccny.cuny.edu

The objective of this minireview is to summarize our recent findings on the importance of porosity of carbons for energy related applications. The examples of the performance of porous carbon in these applications concern ORR and CO₂ electroreduction [13–18]. Even though for these processes surface chemistry is of paramount importance, our results indicate the small pores can contribute markedly to the efficiency of these target processes.

2. CO₂ electroreduction

There have been numerous works published addressing the applications of nonporous carbon materials such as CNT or graphene as CO₂ electroreduction catalyst. In all these papers the state-of-the-art is that nitrogen incorporated to the carbon matrix [7, 8], especially in a pyridinic configuration, is a crucial center, on which CO₂ reduction of CO₂⁻ intermediate and then to COOH* or CO takes place. This finding was also supported by theoretical calculations [19].

Following the mentioned above findings, and knowing that carbon pores are built of disturbed graphene layers [20], we have chosen for first experiments the carbon derived from polystyrene sulfonic acid-co maleic acid sodium salt [21]. To

introduce nitrogen groups, the carbon was impregnated with urea and heated at 800 °C [13]. That treatment resulted in the introduction of 3.2 at.% nitrogen to the surface, mainly in pyridine and quaternary nitrogen. The sample without nitrogen was referred to as S-doped polymer-derived carbon (CPS) and with nitrogen as S,N-doped polymer-derived carbon (CPSN). For comparison, the experiments were also run on commercial BAX-1500 wood-based carbon sample. The parameters of porous structure are presented in Table 1.

The CO₂ electroreduction was run in 3-electrode cell in 0.1 M KHCO₃ as an electrolyte that was purged with CO₂ before the reduction process. The chronoamperometry was run at various potentials to determine the potential at which the maximum Faradaic efficiency (FE), for CO was found. The best results were obtained on CPSN carbon on which FE was 11.3% (Fig. 1A). Interestingly, methane was also detected on this carbon with FE of ~0.20% (Fig. 1B). Methane has never been detected previously on nonporous carbons. Detailed surface characterization of all carbons tested in this approach suggested that the porosity might have helped with CO₂ reduction via increasing its adsorption strength and thus promoted the electron transfer and formation of intermediates.

Table 1

The parameters of porous structure for the materials studied.
Reprinted with permission from Ref. [13]. Copyright 2016, Wiley.

Sample	S _{BET} (m ² g ⁻¹)	V _t (cm ³ g ⁻¹)	V _{meso} (cm ³ g ⁻¹)	V _{<0.7 nm} (cm ³ g ⁻¹)	V _{<1 nm} (cm ³ g ⁻¹)	V _{mic} (cm ³ g ⁻¹)	V _{mic} /V _t
CPS	1523	1.354	0.728	0.235	0.398	0.626	0.46
CPSN	1332	1.307	0.740	0.271	0.394	0.567	0.43
BAX	1541	1.074	0.554	0.159	0.277	0.520	0.48

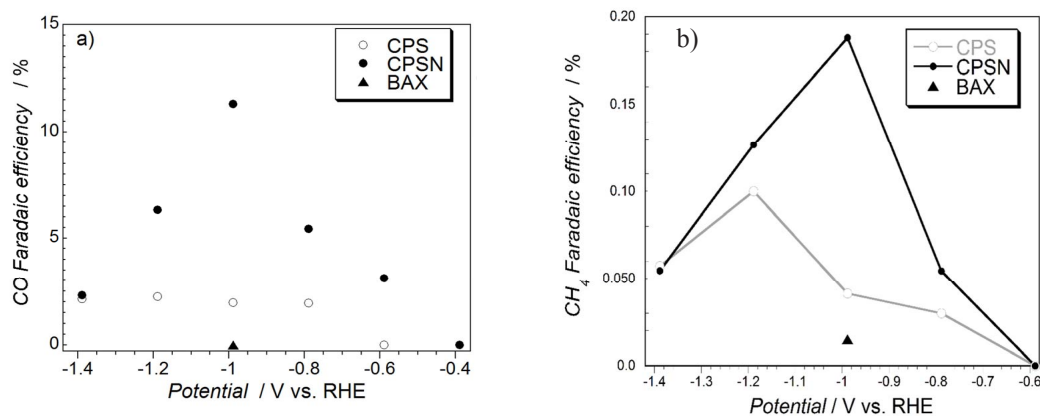


Fig. 1. Faradaic efficiencies for CO (A) and CH₄ (B) formation. Adapted with permission from Ref. [13]. Copyright 2016, Wiley.

As indicated in Table 1, the volume of small pores, $V_{<0.7 \text{ nm}}$, where CO_2 adsorption would be the strongest, was the highest for CPSN. No without significance was its content of nitrogen catalytic centers, which-via providing the positive charge to the surface – enhanced also adsorption of CO_2 intermediate. Those centers, basic in their nature, also resulted in a decrease in the FE of the hydrogen evolution reaction (HER). The polymer derived carbon had a marked volume of large transport pores which helped with mass transfer to the catalytic centers. Unfortunately, the stability of the catalyst was not sufficient and pyridinic groups underwent oxidation to pyridones.

Encouraged by those results, we have introduced nitrogen to the surface of BAX carbon by a thermal treatment with melamine (denoted as M; oxidation denoted as O) [14]. Interestingly, one sample's porosity, that of BAX-M-950 (the last three digits represent the temperature of heat treatment) resembled very closely the porosity of BAX carbon heated at 950 °C (Table 2). Since the melamine treatment introduced 4.8 at.% nitrogen to the surface, the effect of chemistry could be separated from those of pore sizes and volumes. The electrochemical CO_2 reduction at -0.86 V vs. RHE (reversible hydrogen electrode) on the modified sample showed about 20% FE for CO formation and it was stable for 24 h of the reduction process (Fig. 2). Methane was also formed with about 0.7% FE. Since for the first 4 h of reduction an increase in FE was found, and assuming that the reduction process can be beneficial for FE, the samples were reduced in an electrolyte saturated with N_2 at -0.86 vs. RHE . This resulted in a 100% improvement in FE for both CO and CH_4 (Fig. 2). It was also found that FE for H_2 was 40% and thus in this way gas resembling syngas for further chemical synthesis was formed. The surface chemistry of the catalyst was very stable and only slight effect of oxidation was found (Fig. 3a). The blank tests showed that

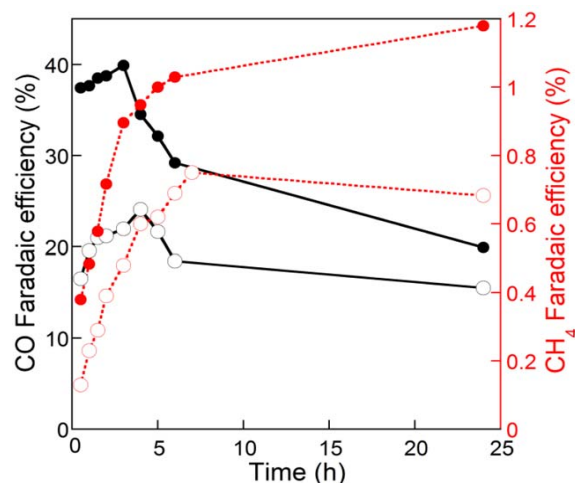


Fig. 2. The FE for CO and CH_4 measured on BAX-M-950. Open symbol-initial sample; closed symbol – after 4 h of reduction at -0.86 vs. RHE in N_2 saturated electrolyte).

the decomposition of carbon surface leading the either CO or CH_4 had a negligible effect on FEs. Ash presented in the samples (2%), was found as not determining the catalytic performance. The most important were pyridinic groups and FE for CO formation showed a linear dependence on the amount of these groups on the carbon surface (Fig. 3b).

The amount of methane formed showed linear dependence on the amount of CO detected (Fig. 3C). It was proposed that methane formation was not an entirely electrochemical process (requires 8 electrons). The small pores/ultramicro-pores of carbon have a potential to work as pseudo Fisher-Tropsch nanoreactors. For a classical Fisher Tropsch process, high pressure of CO and H_2 is needed along with active sites of a catalyst, on which C-O bond is split and hydrogenation occurs. In our system both CO and H_2 co-existed and were formed at the same potential. Their adsorption in small pores might have resulted in high pressure leading to the bond splitting and hydrocarbon formation. That hypothesis needs further testing.

Table 2

The parameters of the porous structure for the carbon modified with melamine. Reprinted with permission from Ref. [14]. Copyright (2017) Elsevier.

Sample	S_{BET} (m^2/g)	V_t (cm^3/g)	V_{meso} (cm^3/g)	$V_{<0.7 \text{ nm}}$ (cm^3/g)	$V_{<1 \text{ nm}}$ (cm^3/g)	V_{mic} (cm^3/g)	V_{mic}/V_t
BAX-950	1533	0.951	0.509	0.110	0.201	0.442	0.46
BAX-O-950	1404	0.811	0.377	0.084	0.207	0.434	0.54
BAX-M-950	1494	1.032	0.637	0.146	0.195	0.395	0.38
BAX-M-950-O	1440	0.995	0.611	0.145	0.198	0.384	0.39

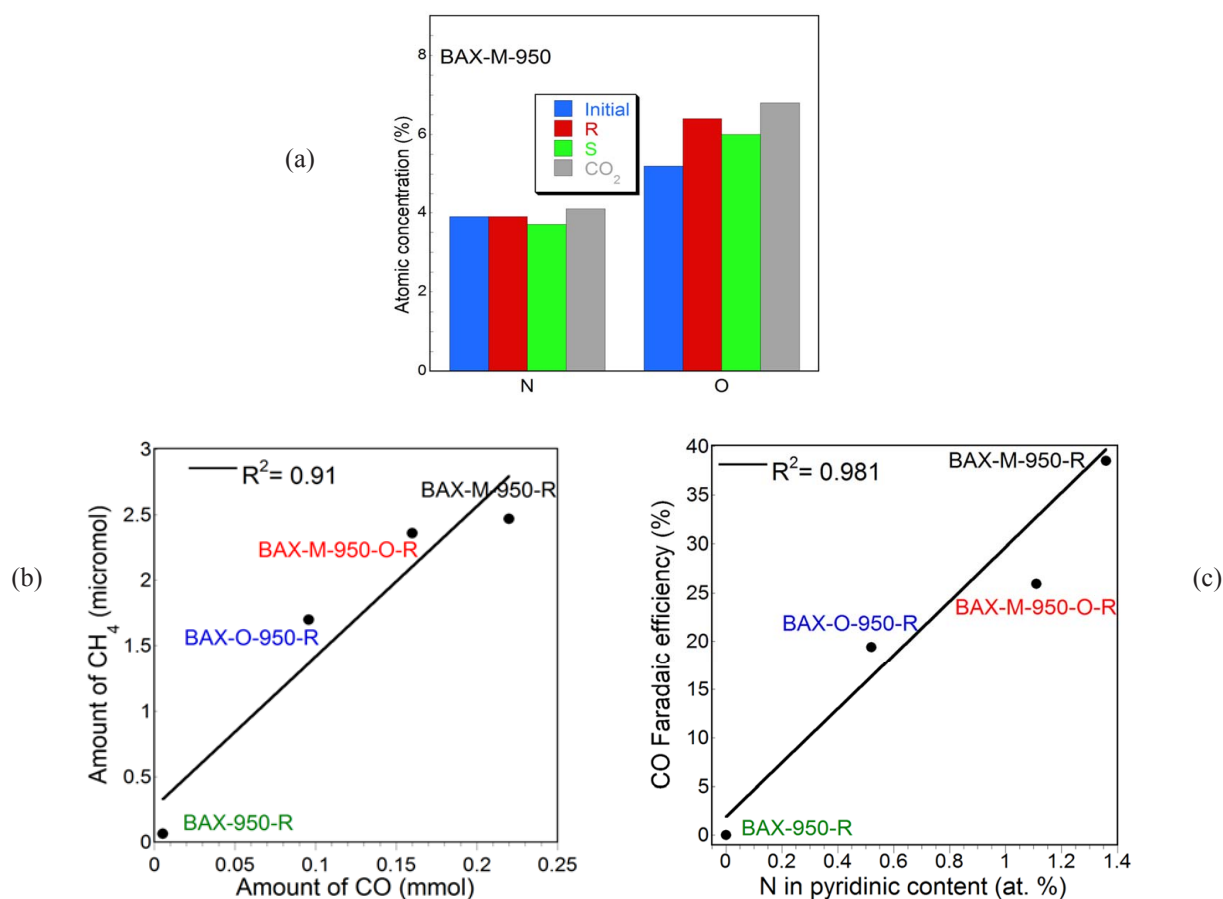


Fig. 3. A) Nitrogen and oxygen content on the surface of the initial sample, reduced in N₂ saturated electrolyte – R; Stabilized in N₂ saturated electrolyte – S and after CO₂ electroreduction – CO₂; B) Dependence of CO FE on the content of nitrogen in pyridinic groups; C) Dependence of the amount of CH₄ formed on the amount of CO formed. Reprinted with permission from Ref. [14]. Copyright 2017, Elsevier.

3. Oxygen reduction reaction (ORR)

Another important energy-related process is that of oxygen reduction on a fuel cell cathode. So far, the best catalyst has been Pt/C, however, its high cost and intolerance to methanol crossover prompted research efforts on the development of new efficient catalysts. Carbon nanomaterials, such as CNT or graphene were the first to be tested [7]. It has been established that nitrogen and sulfur heteroatoms, when introduced to the carbon matrix in condensed rings, create positively charged sites on which oxygen reduction takes place [22]. Numerous papers on nitrogen or nitrogen and sulfur modified carbon have reported the number of electrons transfer close to 4 and similar to that on Pt/C (more efficient), however the onset potential in majority of works was still less positive than on Pt/C [8]. Even though on Pt/C the kinetic current density is higher than on nitrogen-doped carbon materials, the latter have a major advantage of being resistant to methanol crossover and of having a high electrochemical stability.

Even though some ordered mesoporous carbons, but only those doped with nitrogen, have been studied as ORR catalysts [23–26], the micropore effect have not gotten sufficient attention. Larger pores were priced as providing a fast mass transfer to N-containing catalytic sites and in the majority of cases n was close to 4 and kinetic current reached 5 mA/cm². The onset potential was still less positive than that on Pt/C.

To further study in more details the effect of carbon surface on ORR we have performed the ORR experiments in alkaline electrolyte on the series of microporous carbons with hydrophobic ultramicropores derived from polyHIPE (polymerized High Internal Phase Emulsion) [17]. They had traces on nitrogen on the surface (<0.5 at.%) and 8–10 at.% oxygen, mainly in epoxy group. The three carbons tested, CFAT-A, CFAT-B and CFAT-C, had volumes of ultramicropores of 0.135, 0.187, and 0.253 cm³/g, respectively (Fig. 4). All of them show marked oxygen reduction hump (Fig. 5). The electrochemical tests results collected in Fig. 6 showed the number of electron transfer

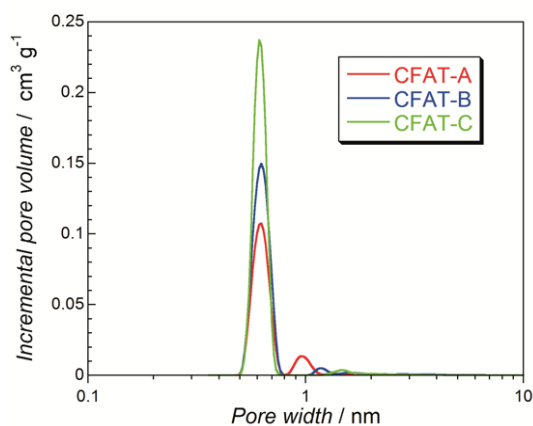


Fig. 4. Pore size distribution for polyHIPE derived carbons. Reprinted with permission for Ref. [17]. Copyright 2016, American Chemical Society.

close to 4, which increased with an increase in the volume of small pores. The onset potential, although still lower than that on Pt/C, also showed an increasing trend with an increase in $V_{<0.7 \text{ nm}}$.

The same was found for the kinetic current normalized per unit surface area (Fig. 7A). In-

terestingly, the dependence of the kinetic current density at various potentials on the volume of ultramicropores was also found and that dependence was stronger at more positive potentials (Fig. 7B). This results clearly indicated that ORR with a high efficiency can happen on microporous carbons and mechanism can be different than that proposed on carbons modified with nitrogen or sulfur. The results suggested that ultramicropores of hydrophobic nature can attract/withdraw oxygen from aqueous electrolyte owing to a higher affinity of oxygen to those pores than to water. Then oxygen is strongly adsorbed in those pores owing to the overlapping of adsorption potentials and this process, combined with the applied potential, results on O-O bond splitting and acceptance of 4 electrons with formation of OH^- with an involvement of water molecules present at the entrance of the pores. The latter has higher affinity to water than to the hydrophobic carbon pores and therefore moves to the liquid phase leaving the pore available to other O_2 molecules dissolved in an electrolyte.

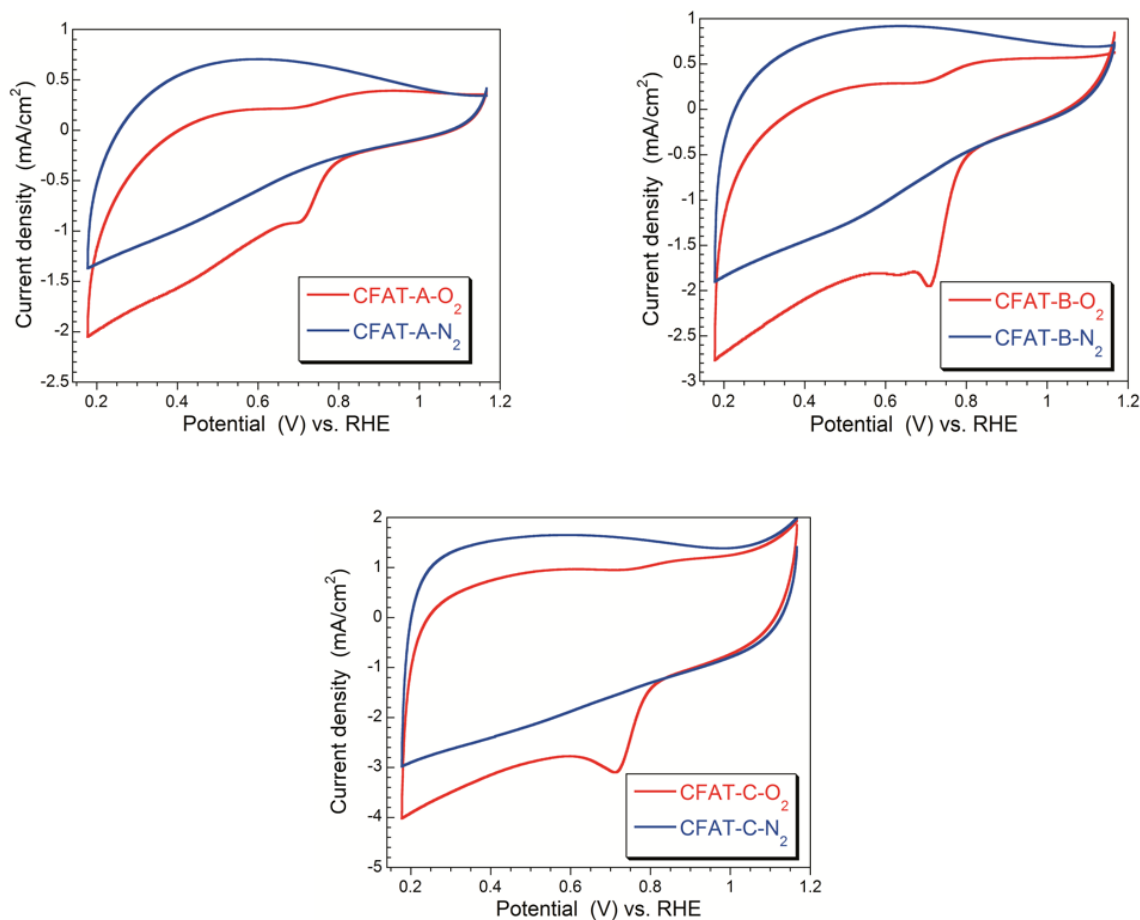


Fig. 5. Cyclic voltammograms on modified glassy carbon RDE in 0.10 M KOH at scan rate of 5 mV/s for the materials studied. Reprinted with permission for Ref. [17]. Copyright 2016, American Chemical Society.

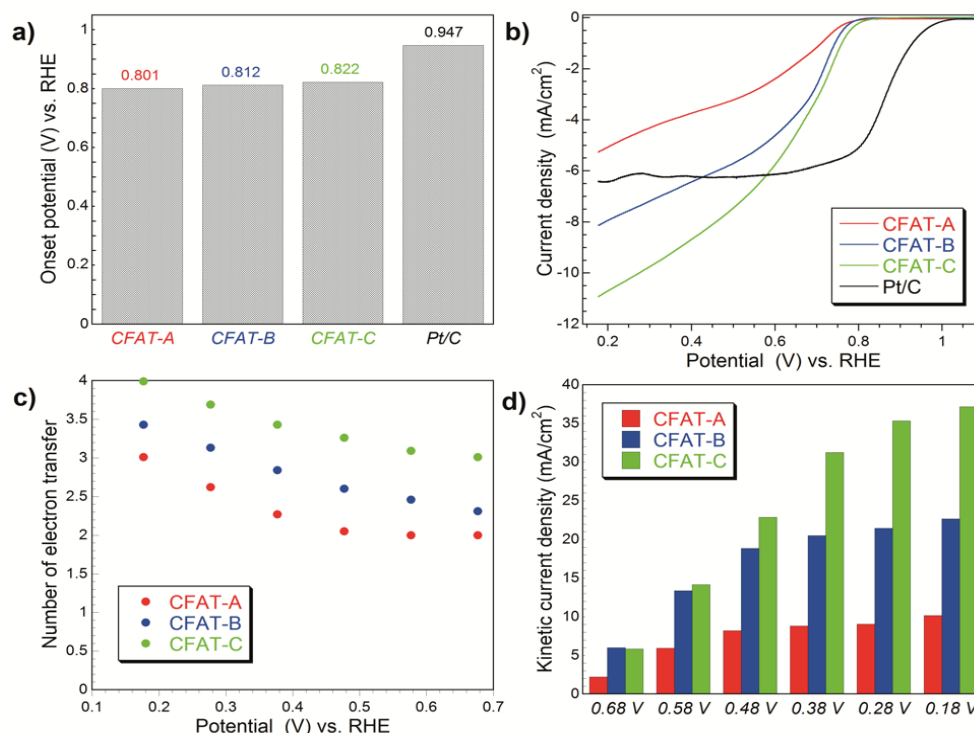


Fig. 6. a) Onset potentials; b) Linear sweep voltammograms on the modified glassy carbon RDE in O_2 -saturated 0.10 M KOH at 2000 rpm and scan rate of 5 mV/s; c) Number of electron transfer versus potential and d) Kinetic current density for the materials studied. Reprinted with permission for Ref. [17]. Copyright 2016, American Chemical Society.

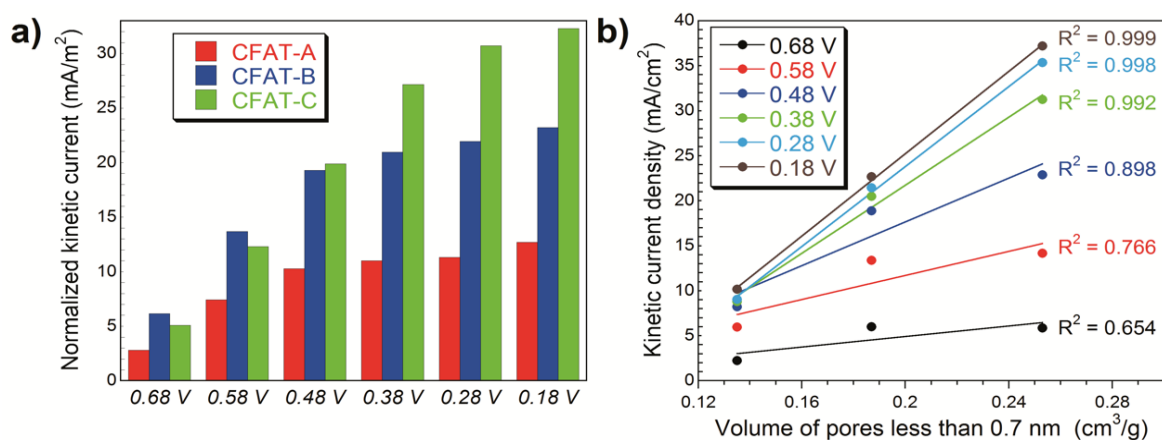


Fig. 7. a) Normalized kinetic current densities per S_{BET} surface area of the polyHIPEs carbons; b) Dependence of the kinetic current density vs. volume of pores smaller than 0.7 nm. Reprinted with permission for Ref. [17]. Copyright 2016, American Chemical Society.

To further support our hypothesis, we have performed the experiments on carbon foam (CM) modified with graphite oxide (GO) [18]. The foam had large pores where a deposition of GO flakes could take place. Additionally, the samples were heated at 950 °C to reduce surface/remove oxygen (denoted as H) and modified with sulfur (denoted as -S) and nitrogen (denoted as -N). The carbons had surface areas between 400 and 650 m^2/g and marked volumes of pores with size about 0.6 nm (Fig. 8). Their pH was the basic range and increased with the heat

treatment. The nitrogen content on the surfaces of the N-modified and heat-treated samples reached 3.7% and the surface oxygen content was between 8–20%, depending on the modification applied [18].

The comparison of the cyclic voltammograms curves in electrolytes saturated with nitrogen and oxygen are presented in Fig. 9. For all samples marked oxygen reduction humps are seen. The comparison of onset potentials is presented in Fig. 10A. They are lower than that on Pt/C and marked differences between them were visible.

Interestingly, the most positive potentials were found for S- and N- free carbons and the introduction of GO hydrophilicity to carbon foam decreased the potential in comparison to that on the nonmodified samples. This supported our hypothesis on the importance of hydrophobicity and small pores for the ORR reduction process.

From linear scan voltammetry experiments, the numbers of electron transfer and the % peroxide formed were calculated (Fig. 10 B, C). As for the

onset potential, the best performing samples, which reached the number of electrons transfer 3.94–3.96, were those heteroatom-free. The introduction of S and N to the carbon matrix in fact resulted in a decrease in the ORR efficiency. This was linked to a decrease in the volume of those electrochemically active ultramicropores (Fig. 8). Moreover, as other carbons tested by us in ORR [17], the modified carbon foams showed a high tolerance to methanol crossover and a high cycling stability (Fig. 11).

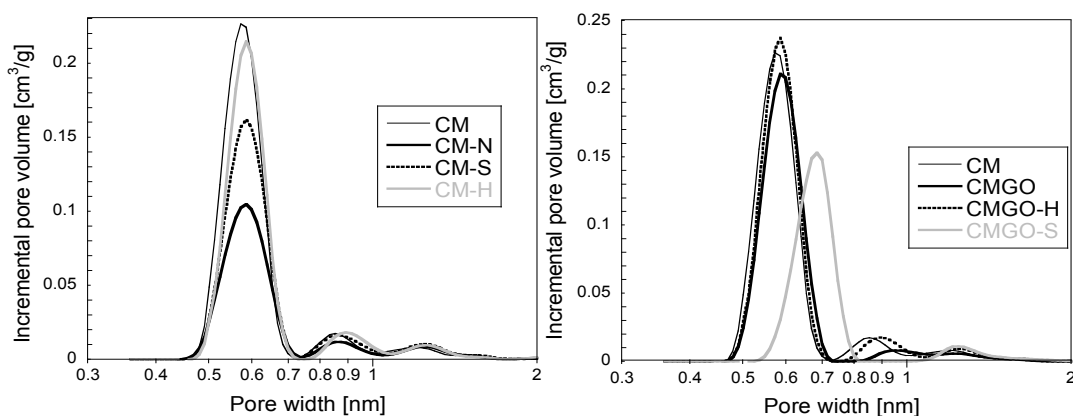


Fig. 8. Pore size distributions for carbon foam (CM) and its modified counterparts. Adapted with permission from Ref. [18]. Copyright 2017, American Chemical Society.

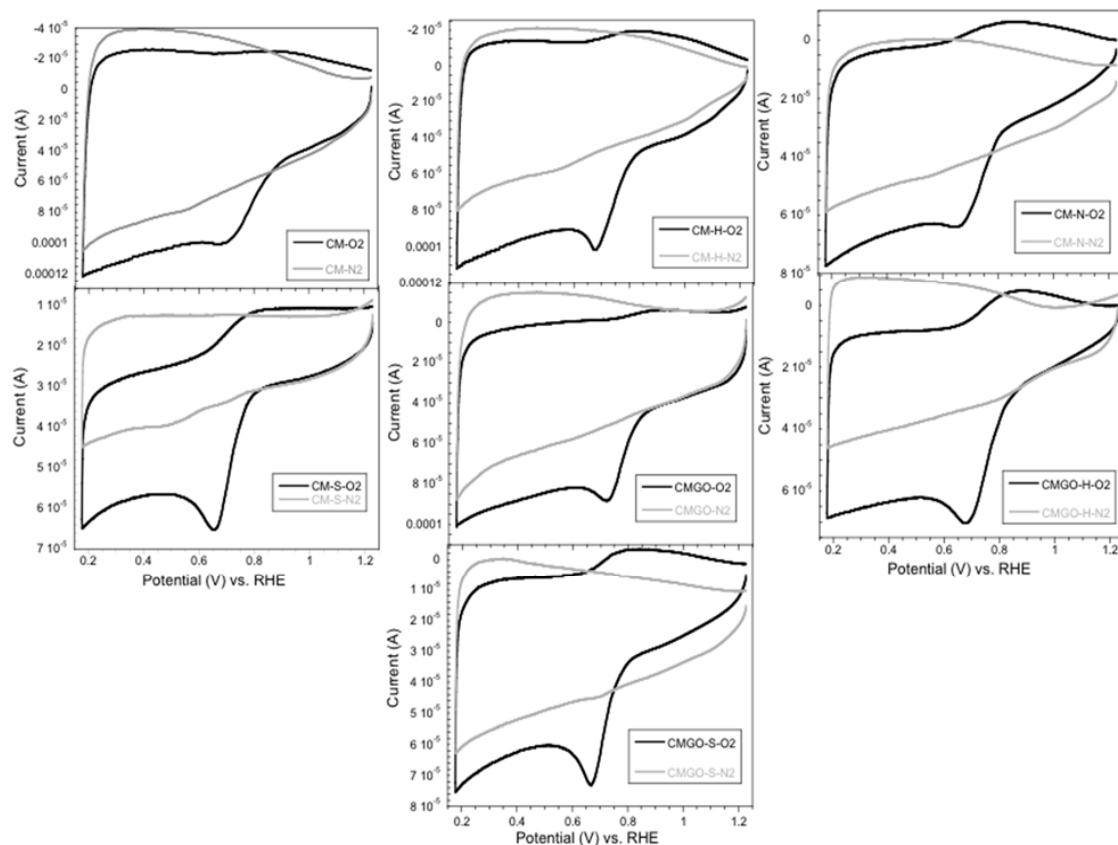


Fig. 9. Cyclic voltammograms measured using rotating ring-disk electrode in 0.10 M KOH at scan rate of 5 mV s^{-1} for the materials studied. Reprinted with permission from Ref. [18]. Copyright 2017, American Chemical Society.

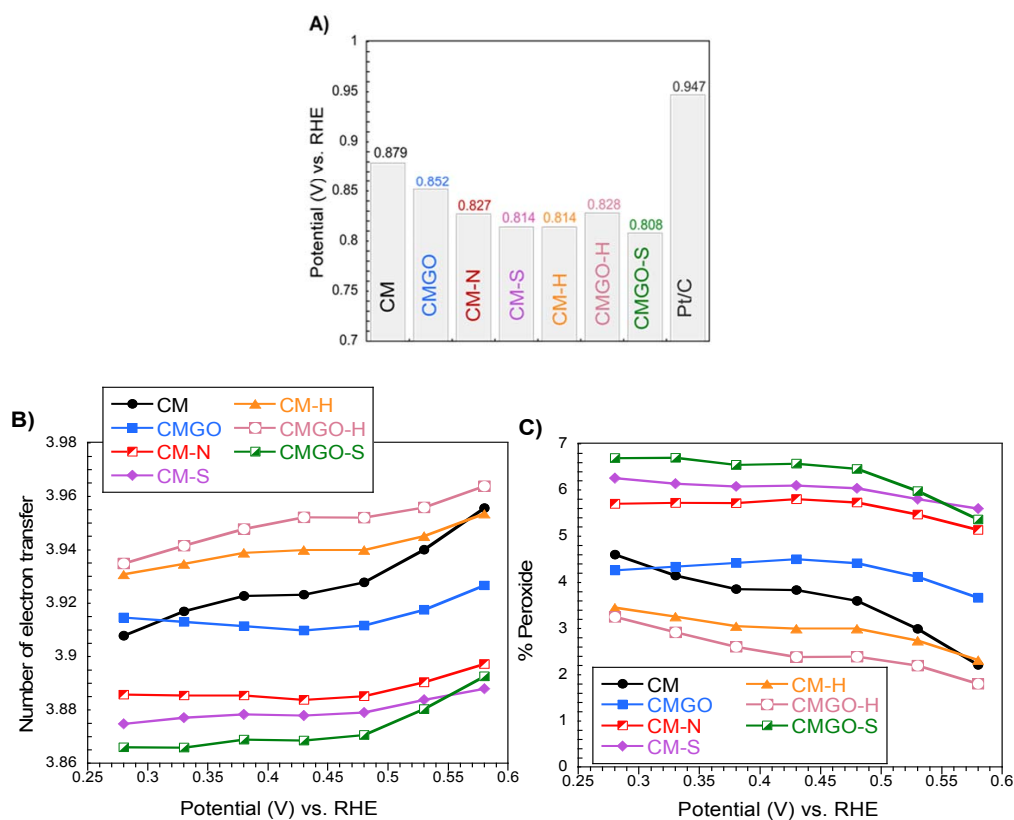


Fig. 10. Comparison of the onset potential (A), number of electron transfer (B) and the percentage of peroxide detected in the cells (C). Reprinted with permission from Ref. [18]. Copyright 2017, American Chemical Society.

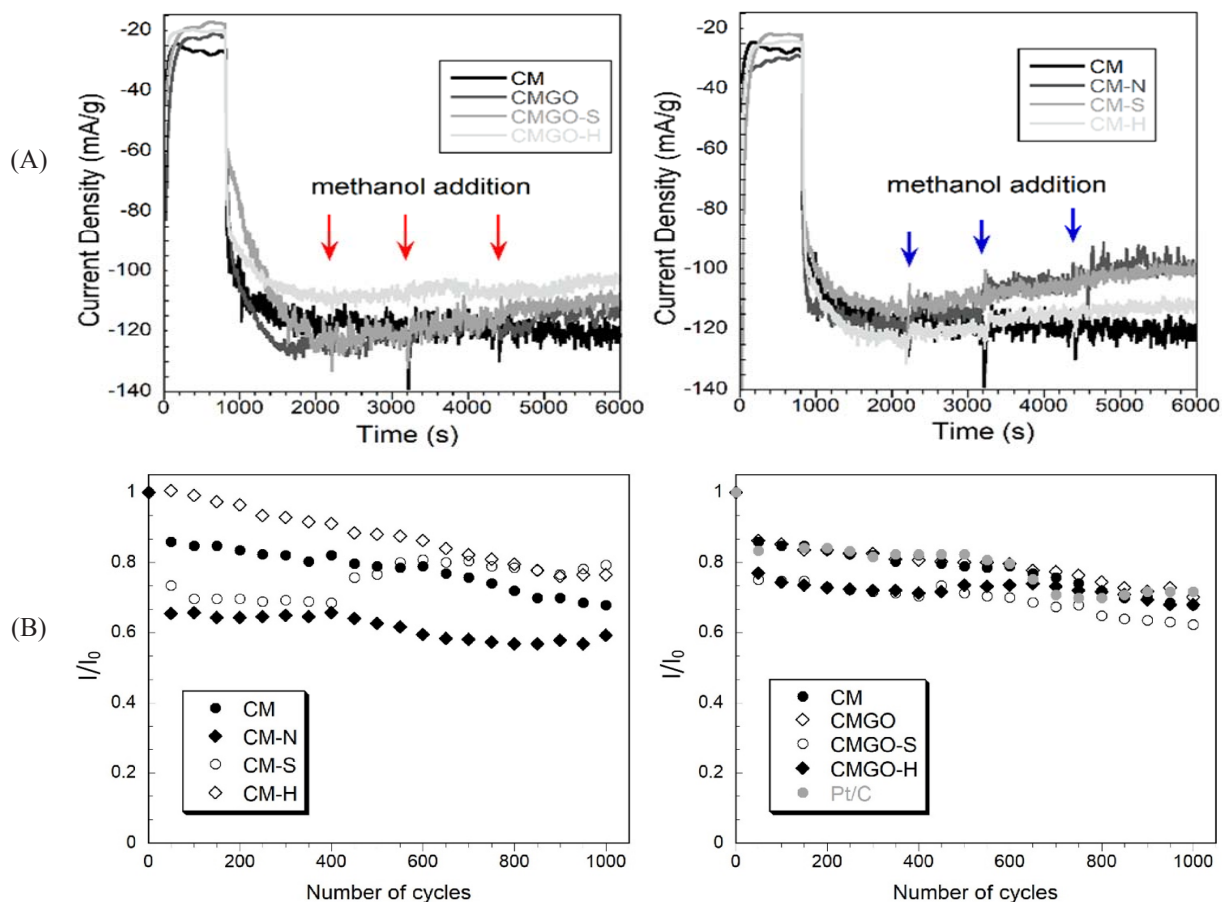


Fig. 11. A) Chronoamperometry response for methanol crossover at the potential of the maximum of the oxygen reduction humps; B) Stability of carbon foam (CM) and its modified counterparts and Pt/C in the ORR over 1000 cycles. Adapted with permission from Ref. [18]. Copyright 2017, American Chemical Society.

4. Conclusions

The results summarized in this minireview suggest that small pores play an important role in an enhancement of the performance of carbons as electrocatalysts of CO₂ and O₂ reduction. They provide strong adsorption forces and the involvement of the adsorption process and strong adsorption potentials have a positive effect on electron transfer processes. There is also a high probability that it helps with bond splitting, which is an intermediate step for both O₂ reduction and transformation of CO to hydrocarbons. In the latter process, small pores with adsorbed CO and H₂ might work as Fisher-Tropsch nanoreactors, where, as a result of high effective pressure, a hydrogen bonding to carbon takes place. Even though the catalytic centers of the carbon matrix related to nitrogen or sulfur are without any doubt important for these reduction reactions, ultramicropores provide an additional mechanism enhancing the overall efficiency of the process.

Acknowledgment

The author is grateful to all students and collaborators listed in Ref. [13–18] for their contributions to this research.

References

- [1]. Von Ostrejko, R. British patent 14, 224, 1900.
- [2]. Von Ostrejko, R. German patent 136, 792, 1901.
- [3]. Von Ostrejko, R. US patent 739, 104, 1903.
- [4]. P. Lodewyckx, Chapter 10, Adsorption of chemical warfare agents. Part of volume: Activated Carbon Surfaces in Environmental Remediation (Ed. Teresa J. Bandosz), *Interface Science and Technology* 7 (2006) 475–528. DOI: [10.1016/S1573-4285\(06\)80019-0](https://doi.org/10.1016/S1573-4285(06)80019-0)
- [5]. M. Zhong, E.K. Kim, J.P. McGann, S.E. Chun, J.F. Whitacre, M. Jaroniec, K. Matyjaszewski, T. Kowalewski, *J. Am. Chem. Soc.* 134 (2012) 14846–14857. DOI: [10.1021/ja304352n](https://doi.org/10.1021/ja304352n)
- [6]. T. Chen, L. Dai, *Mater. Today* 16 (2013) 272–280. DOI: [10.1016/j.mattod.2013.07.002](https://doi.org/10.1016/j.mattod.2013.07.002)
- [7]. Y. Jiao, Y. Zheng, M. Jaroniec, S.-Z. Qiao, *J. Am. Chem. Soc.* 136 (2014) 4394–4403. DOI: [10.1021/ja500432h](https://doi.org/10.1021/ja500432h)
- [8]. X. Liu, L. Dai, *Nature Reviews Materials* 1 (2016) 16064. DOI: [10.1038/natrevmats.2016.64](https://doi.org/10.1038/natrevmats.2016.64)
- [9]. T.J. Bandosz, C.O. Ania, Chapter 4, Surface chemistry of activated carbons and its characterization. Part of volume: Activated Carbon Surfaces in Environmental Remediation (Ed. Teresa J. Bandosz) *Interface Science and Technology* 7 (2006) 159–229. DOI: [10.1016/S1573-4285\(06\)80013-X](https://doi.org/10.1016/S1573-4285(06)80013-X)
- [10]. J. Chmiola, L. Yushin, Y. Gogotsi, C. Portet, P. Simon, P.L. Taberna, *Science* 313 (2006) 1760–1763. DOI: [10.1126/science.1132195](https://doi.org/10.1126/science.1132195)
- [11]. M. Barczak, Y. Elsayed, J. Jagiello, T.J. Bandosz, *Electrochim. Acta* 275 (2018) 236–247. DOI: [10.1016/j.electacta.2018.04.035](https://doi.org/10.1016/j.electacta.2018.04.035)
- [12]. T.J. Bandosz, *Chem. Rec.* 16 (2015) 205–218. DOI: [10.1002/tcr.201500231](https://doi.org/10.1002/tcr.201500231)
- [13]. W. Li, M. Seredych, E. Rodriguez-Castellon, T.J. Bandosz, *ChemSusChem* 9 (2016) 606–616. DOI: [10.1002/cssc.201501575](https://doi.org/10.1002/cssc.201501575)
- [14]. W. Li, B. Herkt, M. Seredych, T.J. Bandosz, *Appl. Catal. B-Environ.* 207 (2017) 195–206. DOI: [10.1016/j.apcatb.2017.02.023](https://doi.org/10.1016/j.apcatb.2017.02.023)
- [15]. W. Li, N. Fechler, T.J. Bandosz, *Appl. Catal. B-Environ.* 234 (2018) 1–9. DOI: [10.1016/j.apcatb.2018.04.021](https://doi.org/10.1016/j.apcatb.2018.04.021)
- [16]. W. Li, T.J. Bandosz, *ChemSusChem* 11 (2018) 2987–2999. DOI: [10.1002/cssc.201801073](https://doi.org/10.1002/cssc.201801073)
- [17]. J. Encalada, K. Savaram, N.A. Travlou, W. Li, Q. Li, C. Delgado-Sánchez, V. Fierro, A. Celzard, H. He, T.J. Bandosz, *ACS Catal.* 7 (2017) 7466–7478. DOI: [10.1021/acscatal.7b01977](https://doi.org/10.1021/acscatal.7b01977)
- [18]. M. Seredych, A. Szczurek, V. Fierro, A. Celzard, T.J. Bandosz, *ACS Catal.* 6 (2016) 5618–5628. DOI: [10.1021/acscatal.6b01497](https://doi.org/10.1021/acscatal.6b01497)
- [19]. P.P. Sharma, J. Wu, R.M. Yadav, M. Liu, C.J. Wright, C.S. Tiwary, B.I. Yakobson, J. Lou, P.M. Alayan, X.S. Zhou, *Angew. Chem. Int. Edit.* 54 (2015) 13701–13705. DOI: [10.1002/anie.201506062](https://doi.org/10.1002/anie.201506062)
- [20]. J. Guo, J.R. Morris, J.Y. Ihm, C.I. Contescu, N.C. Gallego, G. Duscher, S.J. Pennycook, M.F. Chisholm, *Small* 8 (2012) 3283–3288. DOI: [10.1002/sml.201200894](https://doi.org/10.1002/sml.201200894)
- [21]. D. Hines, A. Bagreev, T.J. Bandosz, *Langmuir* 20 (2004) 3388–3397. DOI: [10.1021/la0360613](https://doi.org/10.1021/la0360613)
- [22]. J. Liang, Y. Jiao, M. Jaroniec, S.Z. Qiao, *Angew. Chem. Int. Edit.* 51 (2012) 1–6. DOI: [10.1002/anie.201206720](https://doi.org/10.1002/anie.201206720)
- [23]. Y.-L. Liu, C.-X. Shi, X.-Y. Xu, P.-C. Sun, T.-H. Chen, *J. Power Sources* 283 (2015) 389–396. DOI: [10.1016/j.jpowsour.2015.02.151](https://doi.org/10.1016/j.jpowsour.2015.02.151)
- [24]. Y. He, X. Han, Y. Du, B. Song, P. Xu, B. Zhang, *ACS Appl. Mater. Interfaces* 6 (2016) 3601–3608. DOI: [10.1021/acscami.5b07865](https://doi.org/10.1021/acscami.5b07865)
- [25]. G.A. Ferrero, K. Preuss, A.B. Fuertes, M. Sevilla, M.M. Titritici, *J. Mater. Chem. A.* 4 (2016) 2581–2589. DOI: [10.1039/C5TA10063A](https://doi.org/10.1039/C5TA10063A)
- [26]. M. Kim, H.S. Kim, S.J. Yoo, W.C. Yoo, Y.E. Sung, *J. Mater. Chem. A.* 5 (2017) 4199–4206. DOI: [10.1039/C6TA10679J](https://doi.org/10.1039/C6TA10679J)